



OPEN Simultaneous determination of soil-water characteristic and shrinkage curves of consolidated kaolin under continuous and discrete drying procedures

Hengshuo Liu^{1,2}, Harianto Rahardjo² & Yangyang Li^{3,4}✉

Soil-water characteristic curve (SWCC) and shrinkage curve are essential information required for analyzing the behaviors and properties of unsaturated soils. This study proposes a new method for simultaneous measurement of SWCC and shrinkage curve of a “single” soil specimen. The validation of the method was carried out using kaolin specimens prepared at low levels of consolidation pressures. The changes in void ratio, gravimetric water content, and soil suction of the specimen under continuous or discrete drying procedures were measured using the vernier caliper, the balance, and the osmotic tensiometer, respectively. The results show that the shrinkage curves of all specimens are almost the same regardless of their different initial gravimetric water contents and initial void ratios. However, the obtained gravimetric water content SWCC (SWCC- w) in the lower suction range was related to the initial gravimetric water content of the specimen. In contrast, the degree of saturation SWCC (SWCC- S) of all specimens were almost the same and the air-entry values of different specimens were shown to be quite close. The results indicate that continuous drying procedures would not cause obvious differences in the measured SWCC as well as shrinkage curve compared with the discrete drying procedures. The relationship between the void ratio and soil suction of the specimens shows that the void ratio has a rapid decrease in the lower suction range and reaches the minimum value when the soil suction is about 300 kPa. The proposed method would shorten the time for obtaining the properties of unsaturated soils and would benefit the related analyses.

Keywords Soil-water characteristic curve, Shrinkage curve, Consolidated kaolin, Continuous and discrete drying, Osmotic tensiometer, Void ratio – suction relationship

Soil-water characteristic curve (SWCC) correlates the water content of an unsaturated soil to its soil suction, which is necessary for the study of the behaviors and properties of unsaturated soils such as their permeability, shear strength, and deformation^{1–3}. The water content of an unsaturated soil can be expressed as gravimetric water content (w), volumetric water content (θ), and degree of saturation (S). Thus, various types of SWCC can be deployed for different purposes. The gravimetric water content SWCC (SWCC- w) is the most common type and it describes the mass ratio of water to soil solid at different levels of soil suction, which indicates the water retention capacity of the soil. The volumetric water content SWCC (SWCC- θ) describes the volume ratio of water to the total soil volume at different levels of soil suction. The determination of SWCC- θ requires the soil shrinkage measurement and this type of SWCC is widely used to simulate the transient seepage in unsaturated zones^{4,5}. The degree of saturation SWCC (SWCC- S) describes the volume ratio of water to the pore volume within the soil at different levels of soil suction. SWCC- S also requires the soil shrinkage measurement and it is the most suitable SWCC for the determination of air-entry value (AEV) and estimation of other unsaturated soil properties^{1,6–8}.

¹School of Civil Engineering, Beijing Jiaotong University, Haidian District, Beijing 100044, PR China. ²School of Civil and Environmental Engineering, Nanyang Technological University, Singapore 50 Nanyang Avenue, 639798, Singapore. ³Suzhou Industrial Park Monash Research Institute of Science and Technology, Monash University, Suzhou 215000, PR China. ⁴Department of Civil Engineering, Monash University, 23 College Walk, Clayton, VIC 3800, Australia. ✉email: yangyang.li@monash.edu

Among various types of SWCC, the SWCC- w is the easiest to be measured through many techniques such as centrifuge method, Tempe cell, pressure plate, osmotic control method, filter paper, and WP4C dewpoint potentiometer^{1–3,6,9–12}. A complete SWCC over the full suction range is usually determined by combining several of the above-mentioned techniques due to the limited measuring ranges of each technique. The Tempe cell is installed with a 1-bar ceramic disk and it is usually used to measure the SWCC within 100 kPa suction range. The pressure plate is commonly utilized for SWCC measurement in the suction range below 1500 kPa but the procedure is time-consuming because the low permeable ceramic disk of the pressure plate prolongs the time for equilibrium of the soil specimen under the controlled suction^{1,13,14}. The centrifuge method is much faster than the pressure plate and it can measure SWCC up to several hundreds of kPa, depending on the set-up and maximum rotation rate of the machine^{14,15}. The SWCC in high suction range (i.e., higher than 1500 kPa) is usually measured based on the osmotic control method or using the WP4C dewpoint potentiometer^{16,17}. Finally, the complete SWCC- w over the full suction range can be obtained by plotting the gravimetric water contents against their corresponding soil suctions after combining the data points from various techniques. The soil shrinkage curve is required when determining the SWCC- θ and SWCC- S from the SWCC- w . The shrinkage curve describes the relationship between the void ratio (e) and the gravimetric water content (w) when the soil shrinks in an unsaturated state. To determine the soil shrinkage curve, the change in the volume of the soil specimen when it shrinks is measured so that the specimen's void ratio can be calculated^{8,17,18}. Commonly adopted instruments/methods to measure the volume of the specimen include vernier caliper, 3D scanner, liquid submerging method, and photogrammetry method. Based on the shrinkage curve, the volumetric water content and degree of saturation can be converted from the gravimetric water content.

Usually, the measurement of soil-water characteristic and shrinkage curves was conducted individually, so more than one soil specimen was required for the determination of these two curves. Even though some “identical” specimens were prepared carefully for the measurement, the inadequate combination and/or careless interpretation of the results may still exist and cause further issues when analyzing the unsaturated soil properties^{18–20}. Therefore, a new method that is capable of simultaneously measuring the soil mass, volume, and soil suction of a “single” specimen is required to improve the accuracy and reliability of the measuring results. The soil suction is the most difficult to measure among the three variables. Previous researchers have developed new high-capacity tensiometers (HCTs) with soil suction measuring range exceeding 1500 kPa and designed new set-ups by incorporating the HCT in the measurement of the SWCC and shrinkage curves simultaneously^{18,20,21}. However, the water cavitation issues inside the chamber of HCTs may occur and cause inaccuracy in soil suction measurement, which requires special attentions and operations when using this type of instrument^{22–24}. The experimental results of three types of SWCCs obtained from their new set-ups were not discussed in detail and the relationship between the void ratio and the soil suction were not analyzed.

In this study, kaolin specimens were prepared at different consolidation pressures and used to evaluate the proposed method of simultaneous determination of the soil-water characteristic and shrinkage curves using a “single” kaolin specimen. The “single” kaolin specimen was dried under continuous drying procedures or discrete drying procedures. Meanwhile, the specimen's suction, volume, and mass were measured using the osmotic tensiometer (OT), vernier caliper, and electronic balance in sequence at a time interval of about 12–24 h. The obtained SWCC- w , SWCC- θ , SWCC- S , and soil shrinkage curve of each specimen were compared to analyze the effects of two drying procedures and consolidation pressures on the shape of the curves and the properties of the kaolin specimens. The results validate the accuracy and reliability of the proposed method for the quick determination of soil-water characteristic and shrinkage curves.

Experiments

Preparation of kaolin soil specimens

The index properties of the kaolin used in this study are presented in Table 1. To prepare the soil specimen, the dried kaolin was first mixed uniformly with water at a water content of 80%. The mixed kaolin showed a slurry state at this level of water content.

The mixed kaolin soil was placed in a consolidation ring (63.5 mm in diameter and 19 mm in height) in an oedometer cell. Following ASTM D2435/D2435M (2011)²⁵, different types of kaolin specimens were consolidated by applying different vertical pressure levels of 35.3, 70.6, and 141.2 kPa^{21,26}. For each level of vertical pressure, two kaolin specimens were prepared. After the consolidation, the kaolin specimens were disassembled from the oedometer cell. It can be observed that the height of the kaolin specimens was less than the height of the ring due to the consolidation. The initial mass and volume of the kaolin specimens were recorded for the calculation of their initial gravimetric water content and void ratio. The kaolin specimens were then dried under atmospheric conditions following different drying procedures for the simultaneous determination of soil-water characteristic and shrinkage curves as shown in Fig. 1. The preparation details of kaolin specimens and their drying procedures when measuring the two curves are presented in Table 2.

Specific gravity	2.64
Fines (%)	100
Liquid limit (%)	67
Plastic limit (%)	45
Plasticity index (%)	23

Table 1. Index properties of the kaolin used in this study.

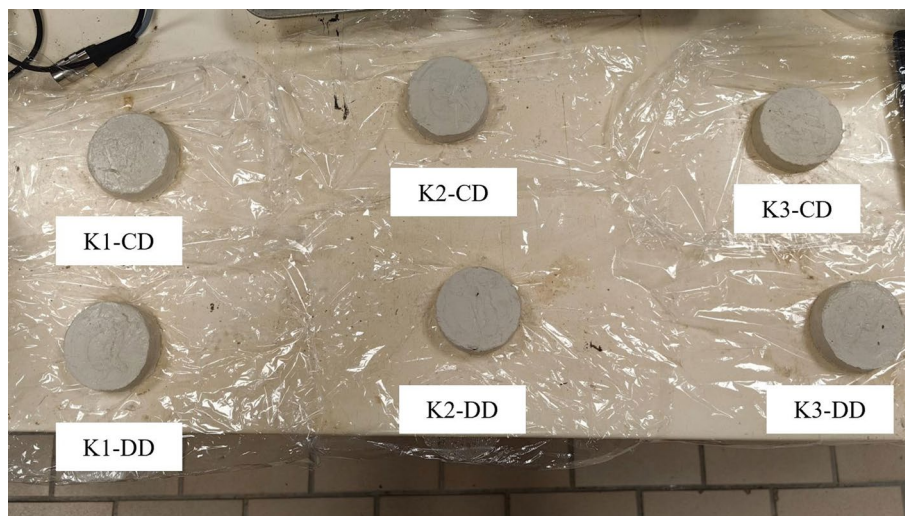


Fig. 1. Prepared kaolin specimens following different drying procedures for simultaneous determination of their soil-water characteristic and shrinkage curves.

Kaolin specimens no.	Vertical pressure level during consolidation (kPa)	Initial gravimetric water content	Initial void ratio	Drying procedures
K1-CD	35.3	58.5	1.55	Continuous drying (CD)
K1-DD	35.3	59.9	1.58	Discrete drying (DD)
K2-CD	70.6	57.7	1.53	Continuous drying (CD)
K2-DD	70.6	57.6	1.52	Discrete drying (DD)
K3-CD	141.2	53.5	1.42	Continuous drying (CD)
K3-DD	141.2	55.6	1.48	Discrete drying (DD)

Table 2. Details of prepared kaolin specimens and their drying procedures to measure soil-water characteristic and shrinkage curves.

Measurement of soil-water characteristic and shrinkage curves of kaolin specimens

In this study, the kaolin specimens prepared at different levels of consolidation pressures as listed in Table 2 were dried under normal atmospheric conditions following continuous or discrete drying procedures. Meanwhile, the mass, dimension, and soil suction of the specimen were recorded for the determination of soil-water characteristic and shrinkage curves. The changes in the mass and the dimensions of the kaolin specimens were recorded using the balance and the vernier caliper, respectively^{1,6}. When using the caliper to measure the dimensions of the specimen, four measurements were taken at different directions of the specimen to obtain the averaged diameter and height of the specimen⁸. The measurement of mass and volume can be finished within several minutes. The soil suction of the kaolin specimens was measured using the osmotic tensiometer (OT) as shown in Fig. 2. The OT was filled with cross-linked polyacrylamide and had a suction measuring range of 1500 kPa^{16,27}. Besides, a high-quality pressure transducer with high precision and fast response was used to prepare the OT to ensure the accuracy of suction measurement in low suction range. The suction of the kaolin specimen was measured by placing the OT in direct contact with the upper surface of the specimen following the measuring procedures proposed by previous researchers^{2,16}. In this study, the soil suction measurement was ensured to be completed within one hour to avoid the interruption on the drying procedures of kaolin specimens. For soil suction measurement using the OT, the soil specimen was sealed with the plastic film to avoid the moisture loss of soil-water from the kaolin specimen as well as the possible change in suction.

As shown in Fig. 3, for the kaolin specimens under continuous drying (CD) procedures (i.e., K1-CD, K2-CD, and K3-CD), the specimen was exposed to the air and the soil-water of the kaolin specimen was left to evaporate from its surface continuously. During the process of water evaporation, the soil suction, volume, and mass of the specimen were measured at a time interval of about 12–24 h. When the soil suction of the specimen was reaching the measuring limit of the OT (i.e., 1500 kPa), the specimen was divided into several pieces: some pieces were completely dried in the oven to determine the gravimetric water content while the others were placed in the containers for the measurement of SWCC in higher suction range using the WP4C dewpoint potentiometer^{2,16}.

In Fig. 3, for the kaolin specimens under discrete drying (DD) procedures (i.e., K1-DD, K2-DD, and K3-DD), to avoid the possible non-uniform distribution of pore-water from the surface to the core of the specimen caused by the air-drying, the specimen was exposed in the air for about 12 h every time and then sealed with the plastic film for 12 h (i.e., discrete drying) to ensure water equalization or uniform pore-water distribution within the specimen before measuring the three variables^{2,20}. Apart from the additional water equalization during the

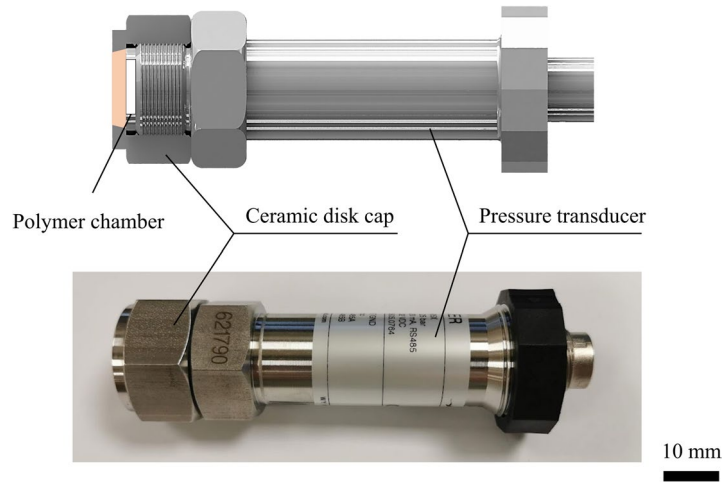


Fig. 2. The osmotic tensiometer (OT) used for fast soil suction measurement.

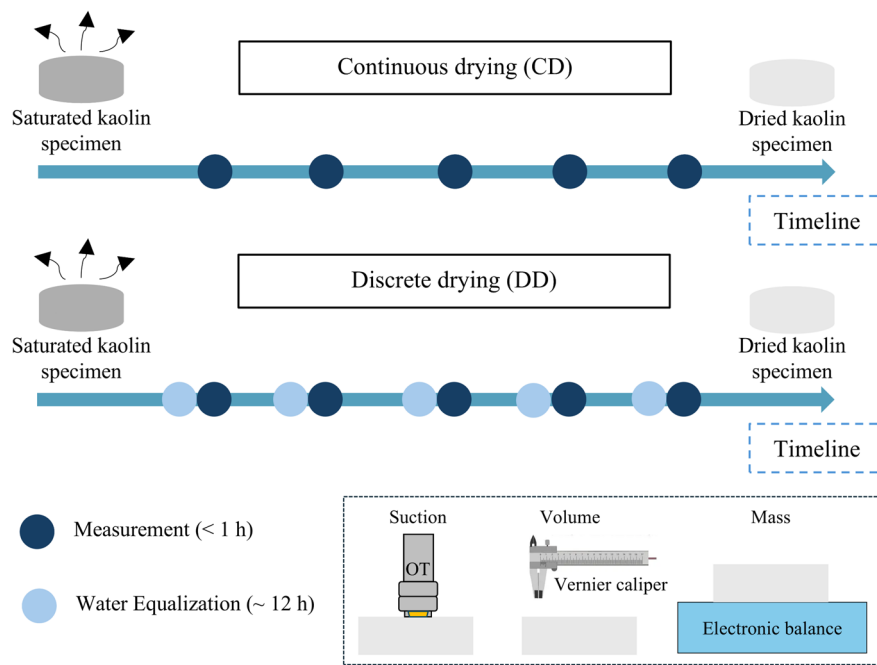


Fig. 3. Schematic description of kaolin specimens under continuous and discrete drying procedures and measurement process using OT, vernier caliper, and electronic balance.

discrete drying procedures, the procedures used for the measurement of mass, volume, and soil suction of the specimens were the same as those for the specimens under CD procedures. However, due to the time required for the water equalization within the specimen, the completion of SWCC and shrinkage curves measurement of the specimen under DD procedures was longer than the specimen under CD procedures.

Best-fitting of soil-water characteristic and shrinkage curves of kaolin specimens

After the completion of SWCC and shrinkage curve measurements of all specimens, the data comprising the gravimetric water content, soil suction, and void ratio of the “single” kaolin specimen were obtained. The void ratio of the specimen was first plotted against its gravimetric water content and best fitted using Eq. (1) to determine the shrinkage curve¹.

$$e = a_{sh} \left(\frac{w^{c_{sh}}}{b_{sh} c_{sh}} + 1 \right)^{\frac{1}{c_{sh}}} \tag{1}$$

where e is the void ratio; w is the gravimetric water content; a_{sh} , b_{sh} , and c_{sh} are three fitting parameters representing the minimum void ratio, the slope of the line of tangency, and the curvature of the shrinkage curve, respectively.

The SWCC- w of the specimen can be plotted directly while the SWCC- θ and SWCC- S were plotted after transforming the gravimetric water content of the specimen into volumetric water content and degree of saturation using Eq. (2) and Eq. (3), respectively¹.

$$\theta = \frac{wG_s}{1 + e} \tag{2}$$

where θ is the volumetric water content; w is the gravimetric water content; G_s is the specific gravity of the kaolin specimen; and e is the void ratio.

$$S = \frac{wG_s}{e} \tag{3}$$

where S is the degree of saturation; w is the gravimetric water content; G_s is the specific gravity of the kaolin specimen; and e is the void ratio.

After plotting the degree of saturation against the soil suction of the kaolin specimens, the data were best fitted using Fredlund-Xing equation shown in Eq. (4) to determine the SWCC- S of the specimens. The air-entry values (AEV) of the kaolin specimens were obtained from the best-fitted SWCC- S curve^{1,8,28}.

$$S(\psi) = C(\psi) \frac{100}{\left\{ \ln \left[e + \left(\frac{\psi}{a} \right)^n \right] \right\}^m} = \left[1 - \frac{\ln \left(1 + \frac{\psi}{\psi_r} \right)}{\ln \left(1 + \frac{10^6}{\psi_r} \right)} \right] \frac{100}{\left\{ \ln \left[e + \left(\frac{\psi}{a} \right)^n \right] \right\}^m} \tag{4}$$

where $S(\psi)$ is the best fitted degree of saturation at the soil suction of ψ ; $C(\psi)$ is the correction factor; ψ_r is a parameter related to residual suction; and a , n , m are three fitting parameters.

Results and discussion

Shrinkage curves of kaolin specimens

The soil shrinkage curves of all kaolin specimens under different drying procedures are presented in Fig. 4. For specimens with the same vertical consolidation pressure, the results show that the specimens under continuous and discrete drying procedures had the same trend of shrinkage. Therefore, the data points from both drying procedures were combined together for the best-fitting of shrinkage curve based on Eq. (1). Figure 4 and Table 2 also show that kaolin specimens prepared at higher consolidation pressures had lower initial gravimetric water

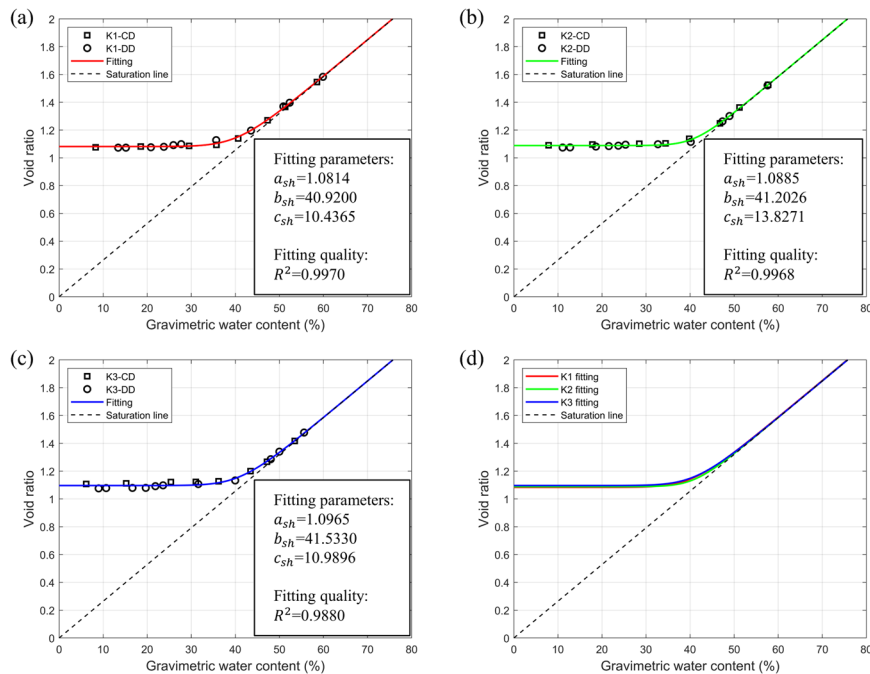


Fig. 4. Shrinkage curves of consolidated kaolin specimens: (a) Shrinkage curve of kaolin specimens prepared at consolidation pressure of 35.3 kPa; (b) Shrinkage curve of kaolin specimens prepared at consolidation pressure of 70.6 kPa; (c) Shrinkage curve of kaolin specimens prepared at consolidation pressure of 141.2 kPa; (d) Summary of shrinkage curves of all kaolin specimens.

contents and lower initial void ratios. The values of a_{sh} obtained from the best-fitted shrinkage curves also show that the minimum void ratios of kaolin specimens under different consolidation pressures are quite similar with the variance less than 0.02. This result is similar with the previous research on the shrinkage curve of kaolin, which proves that different drying procedures would not cause significant difference in the shrinkage curve for the same type of soils⁸. All the kaolin specimens were fully saturated and had the same initial degrees of saturation (i.e., 100%) so that all the curves fall on an identical saturation line. The summary of shrinkage curves of kaolin specimens shown in Fig. 4d indicates that the consolidation process would not affect the complete shrinkage curve of soil specimens, regardless of their different initial gravimetric water content and initial void ratio caused by different levels of consolidation pressures.

Changes in the water content of kaolin specimens with time

All the kaolin specimens under the continuous drying procedure (i.e., K1-CD, K2-CD, and K3-CD) were dried at the same time and the same laboratory environment. The changes in the gravimetric water content of these kaolin specimens are plotted against time in Fig. 5. It shows that the gravimetric water content of all the specimens decreased with time almost linearly. Because the applied vertical pressure on these consolidated specimens increased from K1-CD to K3-CD, the initial gravimetric water content of these specimens decreased from K1-CD to K3-CD. The gradient of the fitting curves describes the rate of gravimetric water content change of the specimens. It shows that the specimen with a higher initial gravimetric water content (i.e., K1-CD) has a relatively higher rate of water content change (0.4504%/h). This may be explained by the surface area of the specimen exposed to air during the continuous drying procedure: the specimen prepared at a lower consolidation pressure (i.e., K1-CD) has a relatively larger volume and larger surface area, resulting in faster evaporation of soil-water as reflected by the higher rate of water content change.

It can also be seen from Fig. 5 that the gravimetric water content of all specimens under the continuous drying procedure were below 5% after the 5-day (i.e., 120 h) of air-drying, indicating that the SWCC and shrinkage curve measurement can be completed within one week. Compared with conventional methods (e.g., pressure plate and filter paper) that require lengthy equilibrium process during SWCC measurement, the proposed method is much faster for measuring the SWCC and shrinkage curve^{1,14}.

Based on the parameters of best-fitted shrinkage curves shown in Fig. 4, the changes in the volumetric water content and the degree of saturation of the kaolin specimens are plotted against time in Fig. 6a,b respectively. The results show that the changes in the volumetric water content and the degree of saturation of the specimens did not follow a linear trend, especially in the beginning of the observation period, compared with the linear changes in the gravimetric water content as presented in Fig. 5. This agrees well with the shrinkage process of the specimens where the specimen shrinks as its gravimetric water content decreases continuously until a minimum void ratio of the specimen is reached as shown in Fig. 4. When the gravimetric water content of the kaolin specimen was about 30%, the shrinkage limit of kaolin specimens was reached. After that, its volumetric water content and degree of saturation started to show a linear relationship with its gravimetric water content as indicated in Eqs. (2) and (3) because the void ratio was a constant (i.e., the minimum void ratio). As a result, its volumetric water content and degree of saturation would decrease with time almost linearly. It can be seen from Fig. 6b that K3-CD started to desaturate at the beginning of the drying procedure. The initial gravimetric water

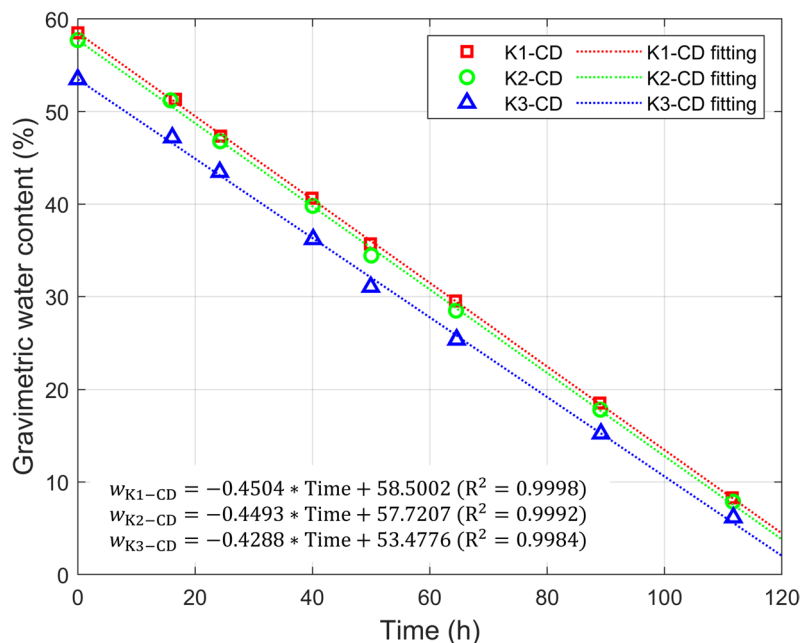


Fig. 5. Changes in the gravimetric water content of kaolin specimens under the continuous drying procedure.

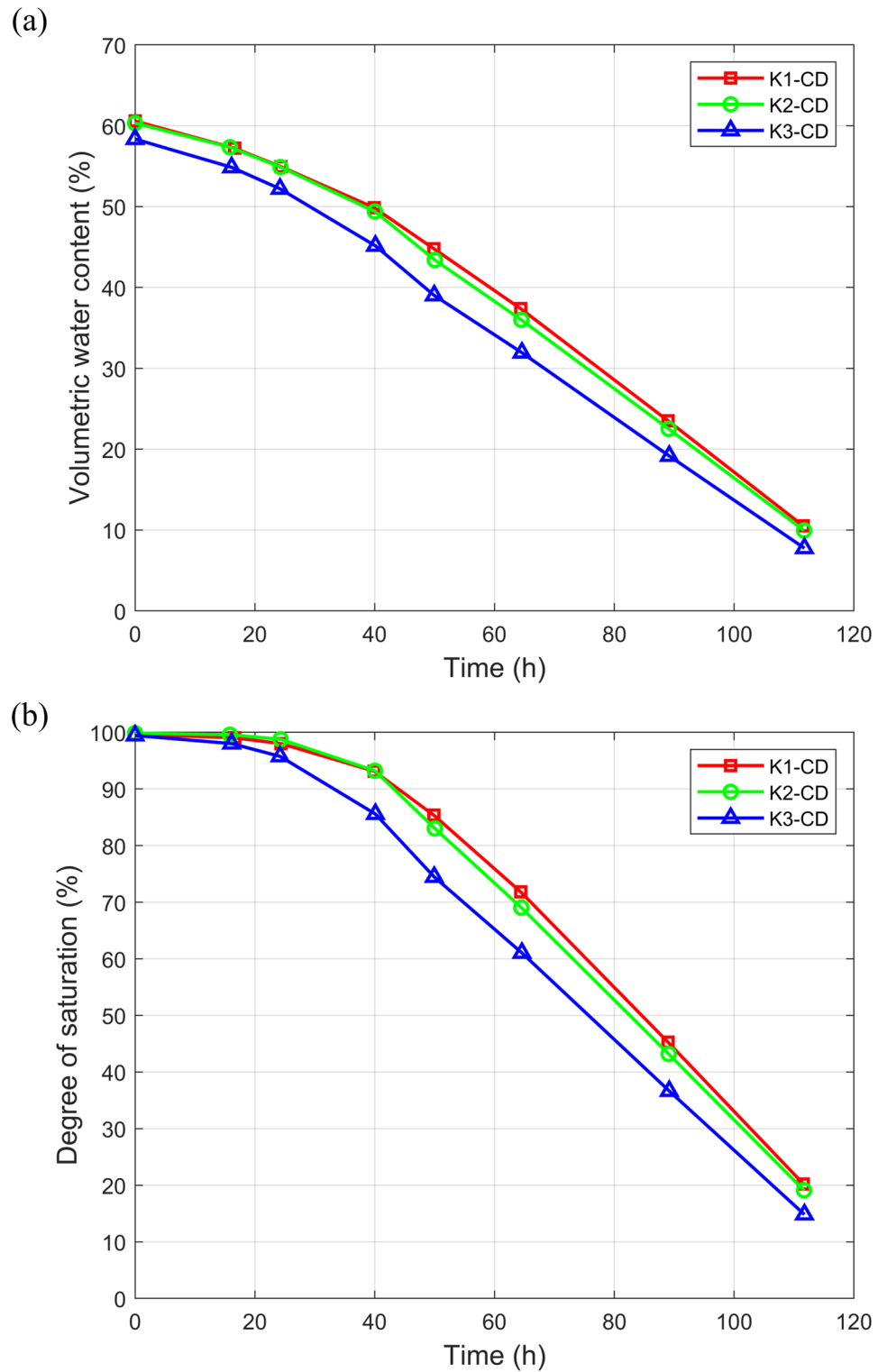


Fig. 6. Changes in (a) volumetric water content and (b) degree of saturation of kaolin specimens under the continuous drying procedure.

contents of K1-CD and K2-CD are higher than that of K3-CD, causing the starting time for the desaturation of these two specimens are behind the specimen of K3-CD.

Soil-water characteristic curves of kaolin specimens

The soil suction of kaolin specimens under the different drying procedures were directly measured using OTs for suctions below 1500 kPa and the WP4C dewpoint potentiometer when the soil suction were beyond 1500

kPa^{2,27}. Based on the measured gravimetric water content and the soil suction of the specimen, its SWCC- w can be plotted. As shown in Fig. 7a, the SWCC in the lower suction range from 0.1 to 100 kPa was highly influenced by the initial gravimetric water content of the kaolin specimen. However, the SWCC of all specimens in the medium suction range (i.e., 100 to 1500 kPa) and the high suction range beyond 1500 kPa are very close to each other. The variation in the initial gravimetric water content of specimens would cause the difficulty in best-fitting of the SWCC, resulting in uncertainty in the determination of the air-entry value (AEV) based on the best-fitted SWCC equation^{8,29}. Therefore, it is necessary to use the shrinkage curve of the specimen that was measured simultaneously with the SWCC- w to determine both the SWCC- θ and the SWCC- S as shown in Fig. 7b,c. The variation in the initial volumetric water content of SWCC- θ as presented in Fig. 7b is not very large as compared with the variation in the initial gravimetric water content of the SWCC- w after taking into consideration of the initial void ratio. The SWCC- S as presented in Fig. 7c demonstrates that all kaolin specimens consolidated at different pressure levels have almost the same trend of SWCC. It would be easier and more accurate to use the data points from SWCC- S for best-fitting and determination of the AEV of the different kaolin specimens.

The results of SWCC also show that the data points of the kaolin specimens under continuous drying procedures are very close to those under discrete drying procedures. This indicates that the continuous drying procedures would not cause significant non-uniform water content distribution within the specimen or the large suction gradient within the specimen. Therefore, the suction near the surface of the specimen as measured by the OT is still capable of representing the suction for the entire specimen. Thus, the determination of SWCC of unsaturated soils based on the continuous drying procedures described in this study can be adopted provided that the mild water evaporation process (i.e., under essentially constant room temperature and relative humidity) is maintained in the laboratory. In addition, referring to the changes in the gravimetric water content of the kaolin specimens with time as shown in Fig. 5, the simultaneous determination of SWCC and shrinkage curves using the continuous drying procedures can be completed within one week, which is faster than the discrete drying procedures that can only be completed in about two weeks. However, it should be noted that the rate of water evaporation is also affected by the dimension and surface area of the soil specimen. Therefore, the time for the determination of SWCC and shrinkage curves may vary when taking into consideration of the size and dimension of the soil specimen^{19,20,30}. To summarize, both discrete and continuous drying procedures can be adopted for fast determination of SWCC and shrinkage curve in the laboratory based on the results of this study.

Considering the compatibility of the data points from continuous and discrete drying procedures presented in Fig. 7, these data points were combined for the best-fitting of SWCC- S using Eq. (4). The high R^2 values prove the accuracy and reliability of the method proposed in this study for the simultaneous determination of SWCC and shrinkage curve. The AEV for the soil specimens prepared at different consolidation pressures can be determined from the best-fitted SWCC- S ¹. The results show that the AEV are 168 kPa, 181 kPa, and 180 kPa for specimens prepared at the consolidation pressures of 35.3 kPa, 70.6 kPa, and 141.2 kPa, respectively. The little variation in the AEV of specimens subject to different levels of consolidation pressures shown in this study agrees with previous research on consolidated Regina clay: the AEV of specimens would be consistent if the consolidation pressure applied to the specimens was lower than the AEV¹. A comparison of the best-fitted SWCC- S in Fig. 8d shows that there is no distinct difference among the SWCC- S of specimens prepared at

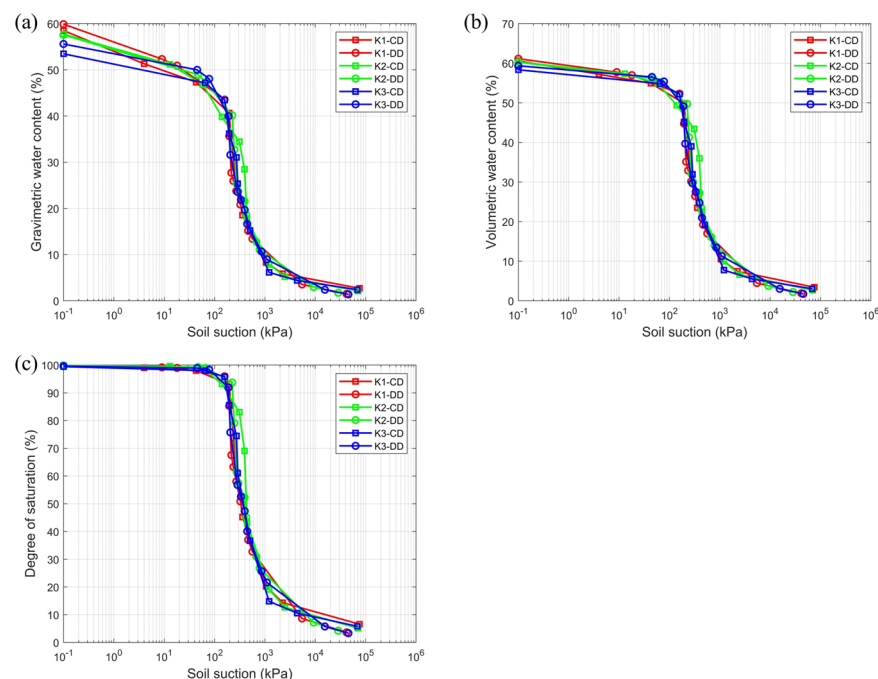


Fig. 7. Summary of SWCCs of all kaolin specimens prepared in this study in different forms: (a) SWCC- w ; (b) SWCC- θ ; (c) SWCC- S .

different levels of consolidation pressures, which indicates that the relatively low levels of consolidation pressures would affect the initial gravimetric water content of the specimens but would not significantly affect the SWCC- S of the unsaturated soils and their AEVs.

Relationship between void ratio and soil suction of kaolin specimens

The void ratio of kaolin specimens prepared at different levels of consolidation pressure are plotted against the corresponding soil suction in Fig. 9. The void ratio shows a rapid decrease in the extremely lower suction range (i.e., 0–10 kPa), which corresponds to the saturated state of the specimens as presented in their shrinkage curves (Fig. 4) and SWCC- w in the lower suction range (Fig. 7). The void ratio gradually decreased in accordance with the increase in the soil suction as well as the decrease in the gravimetric water content. The void ratio finally reached the minimum value when the soil suction was about 300 kPa or the gravimetric water content was about 30% (Fig. 4). This indicates that the higher soil suction (> 300 kPa) would not affect the void ratio or the volume change of the kaolin specimen. As a result, the SWCC or other mechanical properties of the unsaturated soils at high soil suction can be analyzed without considering the volume change when the shrinkage limit of the soil is reached. The relationship between the void ratio and the soil suction helps to analyze and estimate the volume change of the unsaturated soil during the drying process and/or at a specific level of soil suction. Such relationships may vary for different types of unsaturated soils and should be studied further to show the detailed correlation between these two variables. Besides, estimation of the SWCC from the shrinkage curve of the soil could be further studied based on this relationship.

Conclusions

In this study, the new procedures for simultaneous determination of soil-water characteristic and shrinkage curves of a “single” unsaturated soil specimen were proposed and validated by measuring the two curves of kaolin specimens prepared at different levels of consolidation pressures. The void ratio, gravimetric water content, and the soil suction of the specimen during the continuous and discrete drying procedures were measured. The results show that different levels of consolidation pressures would result in different initial gravimetric water contents and initial void ratios of kaolin specimens. However, the shrinkage curves of these specimens are almost the same regardless of their variation in initial gravimetric water content and initial void ratio. The SWCC- w in the lower suction range from 0.1 to 100 kPa was found to be highly affected by the initial gravimetric water content. In contrast, the SWCC- S of all specimens were almost the same and the air-entry values of different specimens obtained from the best-fitted SWCC- S were close to each other. The results also show that the continuous drying procedures would not cause significant difference in the SWCC and shrinkage curve of specimens compared with the discrete drying procedures, provided that the mild water evaporation process (i.e., almost constant room temperature and relative humidity) can be maintained during the measurement of the two curves. The relationship between the void ratio and soil suction of the specimens shows that the void ratio

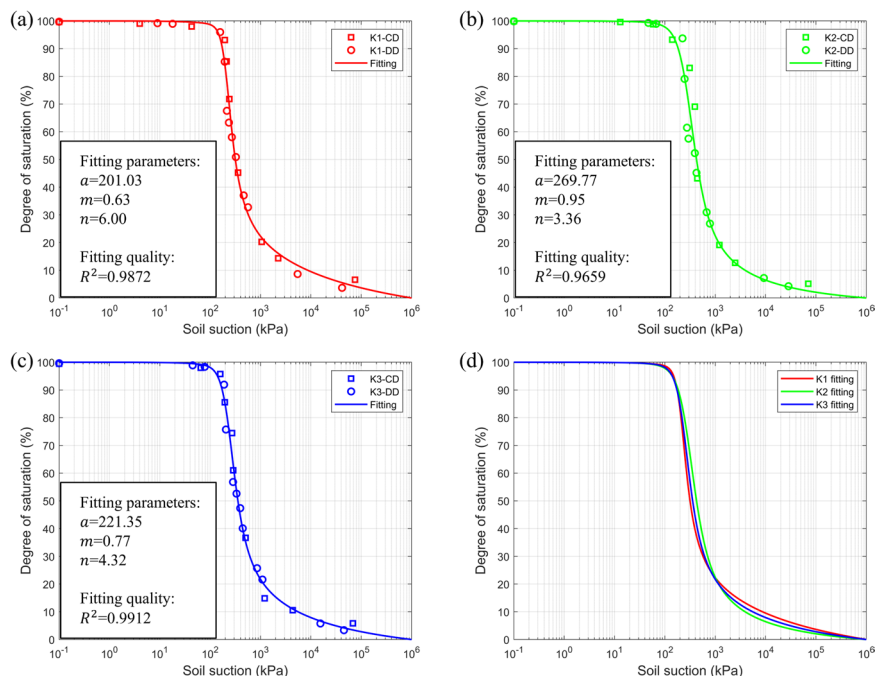


Fig. 8. Best-fitted SWCC- S of consolidated kaolin specimens: (a) Best-fitted SWCC- S of kaolin specimens prepared at consolidation pressure of 35.3 kPa; (b) Best-fitted SWCC- S of kaolin specimens prepared at consolidation pressure of 70.6 kPa; (c) Best-fitted SWCC- S of kaolin specimens prepared at consolidation pressure of 141.2 kPa; (d) Comparison of best-fitted SWCC- S of kaolin specimens prepared at different consolidation pressures.

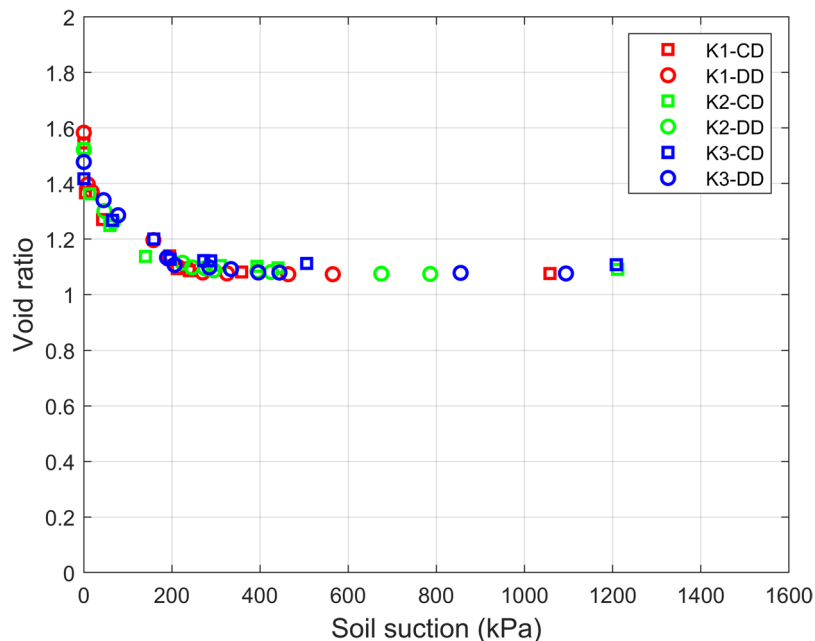


Fig. 9. Relationship between void ratio and soil suction of kaolin specimens.

has a rapid decrease within the extremely lower suction range (i.e., 0–10 kPa) and finally reaches its minimum value when the soil suction is about 300 kPa. In summary, this study proposes a new method for the quick, accurate, and simultaneous determination of SWCC and shrinkage curve of the unsaturated soil, which helps to expedite the process of determining the properties and behaviors of unsaturated soils as well as analyzing related engineering issues associated with unsaturated soils. The proposed procedures should be further evaluated by measuring the SWCC and shrinkage curve of more types of soils such as swelling soils and sandy soils. Besides, the effects of temperature and relative humidity on the measurement should also be analyzed further.

Data availability

The datasets used and/or analysed during the current study available from the corresponding author on reasonable request.

Received: 22 July 2025; Accepted: 9 October 2025

Published online: 14 November 2025

References

1. Fredlund, D. G., Rahardjo, H. & Fredlund, M. D. In *Unsaturated Soil Mechanics in Engineering Practice* (John Wiley & Sons, Inc, 2012).
2. Liu, H., Rahardjo, H., Satyanaga, A. & Du, H. Use of osmotic tensiometers in the determination of soil-water characteristic curves. *Eng. Geol.* **312**, 106938. <https://doi.org/10.1016/j.enggeo.2022.106938> (2023).
3. Mercer, K. & Rahardjo, H. In *Unsaturated Soils Guidelines - Volume 1: Soil Water Characteristic Curves for Materials Classified According To the Unified Soil Classification System* (Australian Centre for Geomechanics, 2019).
4. Leong, E. C. & Rahardjo, H. Two and three-dimensional slope stability reanalyses of Bukit Batok slope. *Comput. Geotech.* **42**, 81–88 (2012).
5. Li, Y., Rahardjo, H., Satyanaga, A., Rangarajan, S. & Lee, D. T. T. Soil database development with the application of machine learning methods in soil properties prediction. *Eng. Geol.* **306**, 106769. <https://doi.org/10.1016/j.enggeo.2022.106769> (2022).
6. Fredlund, D. G. & Rahardjo, H. In *Soil Mechanics for Unsaturated Soils* (John Wiley & Sons, Inc., 1993).
7. Leong, E. C. & Rahardjo, H. Review of Soil-Water characteristic curve equations. *J. Geotech. Geoenviron. Eng.* **123**, 1106–1117 (1997).
8. Wijaya, M., Leong, E. C. & Rahardjo, H. Effect of shrinkage on air-entry value of soils. *Soils Found.* **55**, 166–180 (2015).
9. Delage, P., Howat, M. D. & Cui, Y. J. The relationship between Suction and swelling properties in a heavily compacted unsaturated clay. *Eng. Geol.* **50**, 31–48 (1998).
10. Mendes, J., Gallipoli, D., Toll, D. G. & Tarantino, A. First saturation and resaturation of high capacity tensiometers with 1.5 MPa high air entry value (HAEV) ceramic filters. *PanAm. Unsaturated Soils.* **2017**, 514–522 (2018).
11. Ren, X., Kang, J., Ren, J., Chen, X. & Zhang, M. A method for estimating soil water characteristic curve with limited experimental data. *Geoderma* **360**, 114013. <https://doi.org/10.1016/j.geoderma.2019.114013> (2020).
12. Zeng, Z., Cui, Y. J. & Talandier, J. Investigation of the hydraulic conductivity of an unsaturated compacted bentonite/claystone mixture. *Géotechnique* **72**, 911–921 (2021).
13. Rahardjo, H., Kim, Y. & Satyanaga, A. Role of unsaturated soil mechanics in geotechnical engineering. *Int. J. Geo-Eng.* **10**, 8 (2019).
14. Rahardjo, H., Nong, X., Lee, D., Leong, E. & Fong, Y. Expedited Soil–Water characteristic curve tests using combined centrifuge and chilled mirror techniques. *Geotech. Test. J.* **41**, 207–217 (2018).
15. Khanzode, R. M., Vanapalli, S. K. & Fredlund, D. G. Measurement of soil-water characteristic curves for fine-grained soils using a small-scale centrifuge. *Can. Geotech. J.* **39**, 1209–1217 (2002).

16. Liu, H., Rahardjo, H., Satyanaga, A. & Du, H. Use of synthesised polymers for the development of new osmotic tensiometers. *Géotechnique* **73**, 544–552 (2023).
17. Tripathy, S., Tadza, M. Y. M. & Thomas, H. R. Soil-water characteristic curves of clays. *Can. Geotech. J.* **51**, 869–883 (2014).
18. Najdi, A., Encalada, D., Mendes, J., Prat, P. C. & Ledesma, A. Evaluating innovative direct and indirect soil Suction and volumetric measurement techniques for the determination of soil water retention curves following drying and wetting paths. *Eng. Geol.* **322**, 107179. <https://doi.org/10.1016/j.enggeo.2023.107179> (2023).
19. Bagheri, M. & Rezanian, M. Effect of soil moisture evaporation rate on dynamic measurement of water retention curve with High-Capacity tensiometer. *Int. J. Geomech.* **22**, 04021301 (2022).
20. Lourenço, S. D. N., Gallipoli, D., Toll, D. G., Augarde, C. E. & Evans, F. D. A new procedure for the determination of soil-water retention curves by continuous drying using high-suction tensiometers. *Can. Geotech. J.* **48**, 327–335 (2011).
21. Li, L., Zhang, X. & Li, P. Evaluating a new method for simultaneous measurement of soil water retention and shrinkage curves. *Acta Geotech.* **14**, 1021–1035 (2019).
22. Dainese, R. & Tarantino, A. Measurement of plant xylem water pressure using the high-capacity tensiometer and implications for the modelling of soil–atmosphere interaction. *Géotechnique* **71**, 441–454 (2021).
23. Meghdad, B., Mohammad, R. & Mohaddeseh, M. N. Cavitation in high-capacity tensiometers: effect of water reservoir surface roughness. *Geotech. Res.* **5**, 81–95 (2018).
24. Liu, H., Rahardjo, H., Du, H. & Hamdany, A. H. Long-term decay of the water pressure in the osmotic tensiometer. *J. Rock. Mech. Geotech. Eng.* **15**, 738–746 (2023).
25. ASTM D2435/D2435M. In *Standard Test Methods for One-Dimensional Consolidation Properties of Soils Using Incremental Loading* (ASTM International, 2011).
26. Guan, Y. & Fredlund, D. G. Use of the tensile strength of water for the direct measurement of high soil Suction. *Can. Geotech. J.* **34**, 604–614 (1997).
27. Liu, H., Hamdany, A. H. & Rahardjo, H. Laboratory investigation of osmotic tensiometers filled with cross-linked polyacrylamide. *Transp. Geotech.* **44**, 101173. <https://doi.org/10.1016/j.trgeo.2023.101173> (2024).
28. Fredlund, D. G. & Xing, A. Equations for the soil-water characteristic curve. *Can. Geotech. J.* **31**, 521–532 (1994).
29. Zhai, Q. et al. Prediction of the soil–water characteristic curves for the fine-grained soils with different initial void ratios. *Acta Geotech.* **18**, 5359–5368 (2023).
30. Zhao, Y., Rahardjo, H. & Liu, H. A new experimental setup for the determination of drying soil–water characteristic curve and coefficient of permeability using the continuous evaporation method and osmotic tensiometers. *Soils Found.* **64**, 101470. <https://doi.org/10.1016/j.sandf.2024.101470> (2024).

Acknowledgements

The authors would like to acknowledge the assistance during the experiments provided by the staff of Geotechnics Laboratory, School of Civil and Environmental Engineering, Nanyang Technological University, Singapore.

Author contributions

H. L.: Conceptualization, methodology, formal analysis, data curation, writing—original draft, writing—review and editing. H. R.: Methodology, formal analysis, investigation, writing—review and editing. Y. L.: Methodology, formal analysis, investigation, writing—review and editing.

Declarations

Competing interests

The authors declare no competing interests.

Additional information

Correspondence and requests for materials should be addressed to Y.L.

Reprints and permissions information is available at www.nature.com/reprints.

Publisher's note Springer Nature remains neutral with regard to jurisdictional claims in published maps and institutional affiliations.

Open Access This article is licensed under a Creative Commons Attribution-NonCommercial-NoDerivatives 4.0 International License, which permits any non-commercial use, sharing, distribution and reproduction in any medium or format, as long as you give appropriate credit to the original author(s) and the source, provide a link to the Creative Commons licence, and indicate if you modified the licensed material. You do not have permission under this licence to share adapted material derived from this article or parts of it. The images or other third party material in this article are included in the article's Creative Commons licence, unless indicated otherwise in a credit line to the material. If material is not included in the article's Creative Commons licence and your intended use is not permitted by statutory regulation or exceeds the permitted use, you will need to obtain permission directly from the copyright holder. To view a copy of this licence, visit <http://creativecommons.org/licenses/by-nc-nd/4.0/>.

© The Author(s) 2025